

Selective Probing of the OH or OD Stretch Vibration in Liquid Water Using Resonant Inelastic Soft-X-Ray Scattering

Yoshihisa Harada,^{1,2,*} Takashi Tokushima,³ Yuka Horikawa,^{1,3} Osamu Takahashi,⁴ Hideharu Niwa,^{1,2,5} Masaki Kobayashi,^{2,5} Masaharu Oshima,^{2,5} Yasunori Senba,⁶ Haruhiko Ohashi,⁶ Kjartan Thor Wikfeldt,^{7,8} Anders Nilsson,^{9,10} Lars G. M. Pettersson,¹⁰ and Shik Shin^{1,2,3}

¹*Institute for Solid State Physics (ISSP), University of Tokyo, Kashiwanoha, Kashiwa, Chiba 277-8581, Japan*

²*Synchrotron Radiation Research Organization, University of Tokyo, Sayo-cho, Sayo, Hyogo 679-5198, Japan*

³*RIKEN/SPring-8, Sayo-cho, Sayo, Hyogo 679-5148, Japan*

⁴*Department of Chemistry, Hiroshima University, Higashi-Hiroshima 739-8526, Japan*

⁵*Department of Applied Chemistry, University of Tokyo, Hongo, Bunko, Tokyo 113-8656, Japan*

⁶*JASRI/SPring-8, Sayo-cho, Sayo, Hyogo 679-5198, Japan*

⁷*Science Institute, University of Iceland, VR-III, 107 Reykjavik, Iceland*

⁸*NORDITA, AlbaNova University Center, S-10691 Stockholm, Sweden*

⁹*SUNCAT Center for Interface Science and Catalysis, SLAC National Accelerator Laboratory, 2575 Sand Hill Road, Menlo Park, California 94025, USA*

¹⁰*Department of Physics, AlbaNova University Center, Stockholm University, S-106 91 Stockholm, Sweden*

(Received 15 December 2012; published 8 November 2013)

High-resolution O 1s resonant inelastic x-ray scattering spectra of liquid H₂O, D₂O, and HDO, obtained by excitation near the preedge resonance show, in the elastic line region, well-separated multiple vibrational structures corresponding to the internal OH stretch vibration in the ground state of water. The energy of the first-order vibrational excitation is strongly blueshifted with respect to the main band in the infrared or Raman spectra of water, indicating that water molecules with a highly weakened or broken donating hydrogen bond are correlated with the preedge structure in the x-ray absorption spectrum. The vibrational profile of preedge excited HDO water is well fitted with 50% ± 20% greater OH-stretch contribution compared to OD, which strongly supports a preference for OH being the weakened or broken H-bond in agreement with the well-known picture that D₂O makes stronger H-bonds than H₂O. Accompanying path-integral molecular dynamics simulations show that this is particularly the case for strongly asymmetrically H-bonded molecules, i.e., those that are selected by preedge excitation.

DOI: [10.1103/PhysRevLett.111.193001](https://doi.org/10.1103/PhysRevLett.111.193001)

PACS numbers: 33.15.Fm, 33.15.Mt, 33.20.Rm, 61.25.Em

During the last decade, many studies of water using O 1s x-ray absorption spectroscopy (XAS), x-ray Raman scattering [1–8], and nonresonant x-ray emission spectroscopy (XES) or resonant inelastic x-ray scattering (RIXS) [9–14] have been conducted to provide new information about the local structure of the liquid. The relationship between the local structure of water and the XAS, XES, and RIXS spectral profile is, however, still much debated [6,8,15–23]. In XAS, three characteristic features appear, i.e., preedge at 535 eV, main edge around 537 eV, and postedge near 540 eV. When ice changes to liquid water, the postedge, which has been assigned as due to intact hydrogen bonds (H-bonds), decreases substantially, while the preedge peak, which is interpreted as arising from broken H-bonds, increases [2,3,24]. Theoretical assignments of the spectral features are challenging because the computed XAS profile strongly depends on the model used to describe the core-hole potential [7,8,25–27]. Recently, the degree of H-bond breaking in water has been analyzed as a function of temperature using x-ray Raman scattering [5]. The small (0.9 kcal/mol) enthalpy change estimated from the van't Hoff analysis of the preedge area intensity was claimed to

show the absence of H-bond breaking. Meanwhile, in the x-ray emission spectrum of water obtained by nonresonant (XES) and resonant (RIXS) excitations, two distinct lone pair peaks were observed, and it has been debated whether these peaks represent two distinct local structures of water [6,12,17,20,28,29], one tetrahedrally H-bonded and the other highly distorted, or if they are only manifestations of core hole-induced dynamics producing intact and dissociated species from nearly tetrahedrally H-bonded water [11,18,19].

Here we show high-resolution O 1s RIXS spectra of H₂O, D₂O, and HDO after excitation near the preedge resonance. Figure 1 describes the RIXS process where the electron is resonantly excited from the ground state to the core excited antibonding state localized on a non-H-bonded OH [10,24] and, subsequently, decays back to the original electronic ground state, but with vibrational excitations. These appear due to nuclear motion in the core-excited molecular potential during the lifetime (around 4 fsec [30] for O 1s⁻¹) of the core-excited state and have naturally been interpreted as vibrational or phonon excitations in the ground state potential of the molecule or solid [31,32], permitting direct

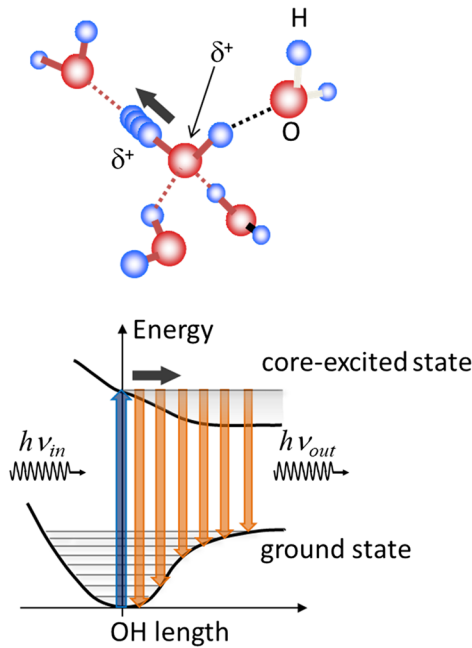


FIG. 1 (color online). A spatial image (upper panel) and schematic of the O 1s RIXS with potential energy description (lower panel) of the accompanying dynamics around the excited water molecule within the lifetime (~ 4 fs for the O 1s core [30]) of the core hole.

comparison to an infrared (IR) or Raman spectrum. Recent high resolution RIXS experiments show the multiple vibrational structure of O₂ [33] and ethylene [34] or excitation of optical phonons in cuprates [35].

An advantage of RIXS over IR and Raman spectroscopy is the possibility to use resonant excitation to selectively probe a subensemble of molecules in a particular type of configuration. Specifically, at the preedge the excitation is into the antibonding O-H σ^* of a weakly H-bonded OH group [2,24]. In this state the excited electron couples weakly to the water conduction band and remains localized on the core-excited molecule longer than the core-hole lifetime [36], which gives an enhanced probability for participator decay where the excited electron fills the core hole with emission near the elastic line. In the O 1s RIXS of water, this low-energy tail of the elastic line at the preedge resonance has been interpreted as due to vibrational excitations from core-hole-induced nuclear dynamics but peaks in this region were not resolved [14]. Using high-resolution RIXS of liquid water, we have now successfully obtained well-isolated multiple vibrational structures at preedge resonant excitation. By analyzing the vibrational energy in comparison to the OH stretch main band of liquid water, we can thus discuss the origin of the preedge structure in the O 1s XAS in terms of the local structural environment in water. Details of the experiment and path integral molecular dynamics (PIMD) simulations are given in the Supplemental Material [37].

Figure 2(a) shows the O 1s XAS of H₂O water (upper right) and a full profile of the ultrahigh-resolution O 1s

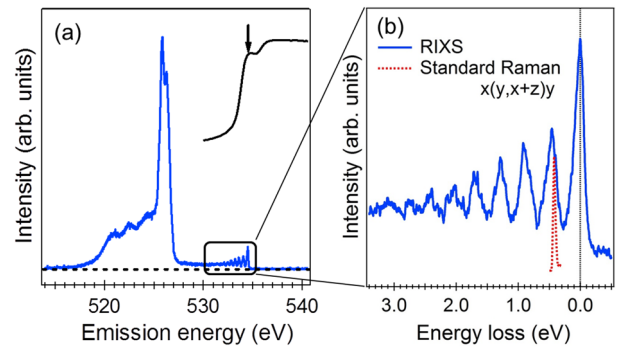


FIG. 2 (color online). (a) O 1s XAS of H₂O (upper right) and O 1s RIXS at preedge excitation as indicated by the arrow. (b) Expanded image of the vibrational structure above 528 eV. Dotted red curve is a standard Raman spectrum of liquid water in the same experimental configuration $x(y, x+z)y$ [39] as the O 1s RIXS.

RIXS (lower left) at XAS preedge excitation as indicated by the arrow. The XAS profile is modified because of saturation effects present in the fluorescence yield mode, which, however, do not affect the RIXS measurements [6]. The emission spectrum below 528 eV corresponds to emission from valence states of H₂O modulated by core-hole-induced dynamics or, equivalently, lifetime-vibrational interference effects [29,38]. The spectrum satisfactorily reproduces previous results [11,12,14] but with much better energy resolution. We focus on the elastic-scattering region above 528 eV, where a small oscillatory structure appears and extends several eV below the elastic-scattering line at 534.5 eV. Here we resolve multiple well-separated vibrational structures with the high energy resolution (0.16 eV), which is better than the vibrational energy of the OH stretch roughly estimated from the peak separation in Fig. 2(b). The profile of each peak is approximately symmetric, and the RIXS spectrum is well fitted with symmetric Gaussians with fixed energy width. The additional curve of $\nu_{0 \rightarrow 1}$ is a standard Raman spectrum of water also at room temperature [39] in the same experimental configuration $x(y, x+z)y$ as the RIXS spectrum for comparison. We note the shift in peak energy between the preedge excited RIXS and the Raman spectrum.

Figure 3 plots, for three experimental runs, the energy separation of the neighboring Gaussian peaks in the overtone region of the vibrational spectrum. The monotonic reduction of the energy separation between the various overtones can be explained by assuming a simple Morse function for the ground state potential energy surface. Most striking is the first vibrational excitation energy ($\nu_{0 \rightarrow 1}$) of 0.45 ± 0.01 eV, which is much closer to the symmetric-stretching mode (0.453 eV) and asymmetric-stretching mode (0.465 eV) of a free water molecule [40] than to the peak position of the IR (0.427 eV) or Raman (0.422 eV) peak [39,41] of pure liquid H₂O, which contains contributions from water molecules in all configurations. It can thus be concluded that the subensemble of water species

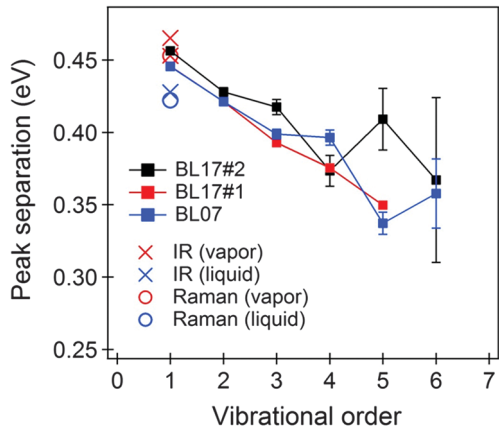


FIG. 3 (color). Energy separation of each neighboring peak in the vibrational RIXS spectrum of H_2O . Three experimental results obtained at different beam lines and beam times are shown to illustrate the small uncertainty in the first excitation energy. The red (blue) denotes gaseous water (liquid water), crosses (circles) denote infrared [41] and Raman [39] experiments.

selected by the preedge excitation corresponds to those having vibrational energies on the blue side of the infrared or Raman OH stretch spectrum, which can be directly interpreted as molecules with a highly weakened or broken donating H-bond. The decreasing energy spacing at higher vibrational order reflects the anharmonicity of the OH stretch vibration. Such a decrease has also been observed in the Raman OH stretch spectra of the first overtone [42].

Similar experiments were also performed with HDO (a 1:1 mixture of H_2O and D_2O giving 2:1:1 HDO: H_2O : D_2O requiring subtracting $\frac{1}{4}$ H_2O and $\frac{1}{4}$ D_2O spectrum contributions) and D_2O using identical conditions as with H_2O [Fig. 4(a)]. The D_2O spectrum indicates smaller vibrational energies than that of H_2O , as expected from the OD-stretching mode energy of D_2O . The mass-dependent isotope effect is a strong evidence for the vibrational origin of the multiple peak structure. Weinhardt *et al.* also demonstrated the isotope effect on the multiple vibrational excitations in the N $1s$ RIXS of aqueous ammonia [43]. In addition, analogous to the case of H_2O , the vibrational energy around 0.34 ± 0.01 eV is closer to the symmetric stretching mode (0.331 eV) and the asymmetric stretching mode (0.346 eV) of a free D_2O molecule [40] than to the main peak of pure liquid D_2O (0.310 eV) [41]. Both the H_2O and D_2O results indicate a strong preference for selection of a highly weakened or broken hydrogen-bond species by the preedge excitation.

Analogous to H_2O and D_2O , the preedge excited state of HDO is localized on an OH or OD group with a highly weakened or broken donating H-bond [24,36]. If the OH and OD groups have equal probability to have a strong or weak H-bond, the x-ray vibrational spectrum of HDO should be reproduced by a one-to-one sum of the H_2O and D_2O spectra. However, as shown in Fig. 4(b), the x-ray vibrational spectrum of HDO is instead well fitted with a weighted sum with ratio OH:OD = 0.76:0.35 = 2.17.

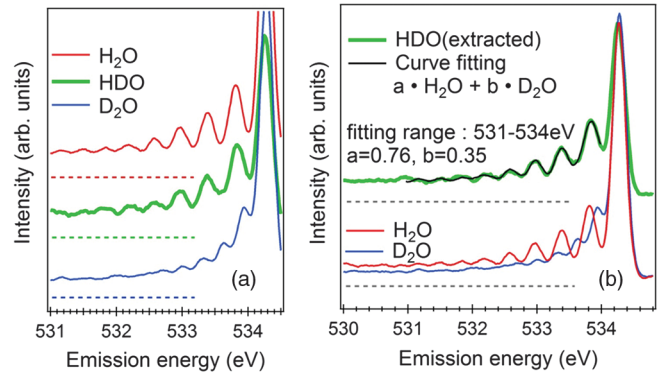


FIG. 4 (color). Isotope effect on the multiple vibrational excitations of water. For each spectrum the background level is indicated by a dashed line. (a) Red and black lines are results for H_2O and D_2O , respectively. The green line is a result for HDO extracted as described in the text. (b) Fitting of the extracted HDO spectrum using a linear combination of the H_2O and D_2O spectra in the range from 531–534 eV.

The preedge in XAS is, however, sharper and at slightly higher energy for D_2O than for H_2O due to the differences in vibrational level spacing [6], which leads to differences in cross section around the preedge for the two isotopes. Taking these differences in excitation probability between the isotopes into account we obtain a ratio of 1.50 ± 0.2 . This strongly supports a preference for OH being the weakened or broken H-bond while preferentially OD produces the H-bond in the species that contribute to the O $1s$ XAS preedge excitation in HDO. This is in agreement with the well-known view that D_2O produces stronger H-bonds than H_2O [44,45] and also supported by our PIMD simulations. Using the cone criterion of Wernet *et al.* [2] with $r_{\text{OO}}^{\text{max}} = 3.3$ Å to define an H-bond we find 42% of the molecules as asymmetric single-donor (SD) species. In this subclass we find 10% more OH than OD as non-H-bonded. Tightening the criterion for an intact H-bond to $r_{\text{OO}}^{\text{max}} = 2.9$ Å while keeping $r_{\text{OO}}^{\text{max}} = 3.3$ Å to define a broken bond, we specifically address more highly asymmetrically H-bonded molecules (52% of the SD species). In this case we find 20% more OH than OD as non-H-bonded showing that the isotope effect becomes more important for the more highly asymmetric species contributing to the preedge. Indeed, the OH stretch of HDO in D_2O is more blueshifted than the OD stretch of HDO in H_2O , as observed in a Raman study by Smith *et al.* [44].

Figure 5(a) shows the excitation energy-dependent vibrational RIXS profile around the preedge of H_2O . Within the experimental resolution, the vibrational peak positions are independent of the excitation energy, indicating the absence of significant variations in the local structure of species contributing to the spectrum near the preedge resonance. There is, however, a variation in the relative intensity of the overtones; below the resonance (531.8 eV), the vibrational excitation was strongly suppressed, while above the preedge excitation (534.5 eV), the peak intensity

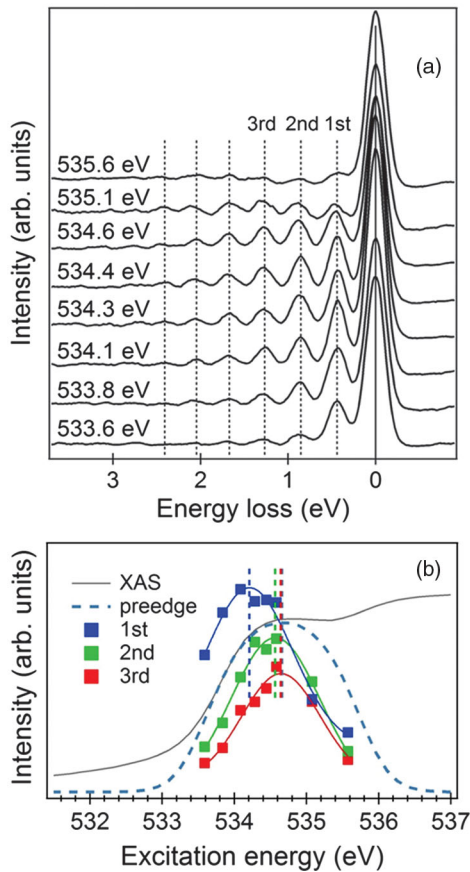


FIG. 5 (color). (a) Excitation energy dependence of the O $1s$ RIXS of H_2O . The elastic peak is taken as reference in all spectra corresponding to zero energy loss. (b) Intensity profile of each vibrational excitation against the excitation energy compared with the O $1s$ XAS of liquid H_2O . Dotted vertical lines indicate the peak position of the Gaussians fitted to each profile. The dotted curve corresponds to the preedge component of the XAS spectrum.

of the higher orders monotonically decreased. However, slightly below the preedge (533.6 eV) the second and higher-vibrational excitation peaks rapidly decreased. These intensity variations result from interference effects when detuning to below the preedge resonance leading to a reduced effective duration time of the scattering process [46]. This will result in a rapid decrease in the peak intensity of higher-order vibrational excitations compared with that of lower ones since the wave packet corresponding to the OH (OD) has less time to evolve in the core-excited state [46]. By plotting the excitation energy dependence of the intensity of each vibrational excitation, it is demonstrated in Fig. 5(b) that the higher-order vibrational excitations have their intensity maximum at successively higher excitation energy. This result can be simply explained by assuming a dissociative potential of the non-H-bonded OH in the resonantly core-excited state [10,47], where the excited system is placed on the sharp slope of the potential energy surface resulting in faster dissociation and increased fraction of higher-order vibrational excitations with increasing excitation energy.

As mentioned above, the vibrational energy is constant across preedge excitation, while the sum of all of the

vibrational components in Fig. 5(b) actually forms the preedge peak. Thus, it can be concluded that the preedge peak in the XAS spectra of water purely originates from a subensemble of species with highly weakened or broken H-bonds. The entire vibrational structure rapidly decreases above the preedge (536.3 eV) and completely disappears at the postedge resonance (540 eV) due to the—compared to the O $1s$ lifetime—much shorter time scale for delocalization of the excited electron in the H-bond-derived conduction band of tetrahedrally H-bonded water [36], leading to the absence of a long-lived excitonic (localized) electron that can contribute to the RIXS elastic channel [36].

Finally, we conclude that at O $1s$ XAS preedge excitation, water molecules with a highly weakened or broken H-bond are definitely selected contrary to what was concluded in a recent study by Pykkänen *et al.* [5], where the weak temperature dependence of the preedge intensity was interpreted as evidence for nonbroken H-bond configurations. However, this apparent contradiction is reconciled by the fact that the total energy cannot be divided into individual H-bond contributions; there are also important contributions from dispersion or van der Waals interactions that become enhanced when tetrahedral structures are broken up leading to closer packing [48]. We would like to stress that the present result is fully consistent with the interpretation of the XES and XAS spectra of ambient water, strongly supporting the two distinct local structure model of ambient water [6,12,20,22,28,49], but the small difference in free energy makes for a challenge to simulations. The current result thus provides additional opportunities for evaluating theoretical models including computing the XAS spectra of water. The OH stretch vibrational energies can then be computed for specific water species in a water model that gives appreciable intensity to the preedge feature.

In summary, we used O $1s$ RIXS spectra to characterize the OH stretch vibrations of the H-bonding properties of the particular subset of molecules in liquid water selected by the strongly debated O $1s$ XAS preedge excitation. On a fundamental level this provides a unique coupling between electronic excitation and vibrational spectral information content of a disordered system such as liquid water. For H_2O and D_2O , $\nu_{0\rightarrow 1}$ coincides closely with the energy of the stretching vibrational mode of gas-phase water rather than that of liquid water, clearly indicating the contribution to the XAS preedge peak of molecules with a highly weakened or broken donating H-bond. Large quantum effects in water are observed with 50% higher contribution of the OH stretch compared to OD to the HDO spectrum supporting a preference for OH being the weakened or broken H-bond in asymmetrically H-bonded species while OD produces the intact H-bond in the species that contribute to the preedge. This trend is well reproduced in PIMD simulations and becomes enhanced for more strongly asymmetrically H-bonded species.

Experiments at SPring-8 BL07LSU were performed jointly by the Synchrotron Radiation Research Organization and the University of Tokyo (Proposals No. 2011B7403,

No. 2012A7403, and No. 2012B7403). Experiments at SPring-8 BL17SU were performed with the approval of the RIKEN SPring-8 Center (Proposal No. 20110058, No. 20120075) and supported by the Japan Society for the Promotion of Science (JSPS) through its Funding Program for World-Leading Innovative R&D on Science and Technology (FIRST) Program. K. T. W. is supported by the Icelandic Research Fund. The PIMD simulations were performed on resources provided by the Swedish National Infrastructure for Computing (SNIC) at the PDC center.

*To whom all correspondence should be addressed.

harada@issp.u-tokyo.ac.jp

- [1] U. Bergmann, Ph. Wernet, P. Glatzel, M. Cavalleri, L. G. M. Pettersson, A. Nilsson, and S. Cramer, *Phys. Rev. B* **66**, 092107 (2002).
- [2] Ph. Wernet *et al.*, *Science* **304**, 995 (2004).
- [3] S. Myneni *et al.*, *J. Phys. Condens. Matter* **14**, L213 (2002).
- [4] J. D. Smith, C. D. Cappa, K. R. Wilson, B. M. Messer, R. C. Cohen, and R. J. Saykally, *Science* **306**, 851 (2004).
- [5] T. Pylkkänen, A. Sakko, M. Hakala, K. Hämäläinen, G. Monaco, and S. Huotari, *J. Phys. Chem. B* **115**, 14 544 (2011).
- [6] A. Nilsson *et al.*, *J. Electron Spectrosc. Relat. Phenom.* **177**, 99 (2010).
- [7] L. Kong, X. Wu, and R. Car, *Phys. Rev. B* **86**, 134203 (2012).
- [8] M. Leetmaa, M. P. Ljungberg, A. Lyubartsev, A. Nilsson, and L. G. M. Pettersson, *J. Electron Spectrosc. Relat. Phenom.* **177**, 135 (2010).
- [9] J.-H. Guo, Y. Luo, A. Augustsson, J.-E. Rubensson, C. Sâthe, H. Ågren, H. Siegbahn, and J. Nordgren, *Phys. Rev. Lett.* **89**, 137402 (2002).
- [10] M. Odelius *et al.*, *Phys. Rev. Lett.* **94**, 227401 (2005).
- [11] O. Fuchs *et al.*, *Phys. Rev. Lett.* **100**, 027801 (2008).
- [12] T. Tokushima, Y. Harada, O. Takahashi, Y. Senba, H. Ohashi, L. G. M. Pettersson, A. Nilsson, and S. Shin, *Chem. Phys. Lett.* **460**, 387 (2008).
- [13] K. M. Lange, M. Soldatov, R. Golnak, M. Gotz, N. Engel, R. Könnecke, J.-E. Rubensson, and E. F. Aziz, *Phys. Rev. B* **85**, 155104 (2012).
- [14] J. Forsberg, J. Gräsjö, B. Brena, J. Nordgren, L.-C. Duda, and J.-E. Rubensson, *Phys. Rev. B* **79**, 132203 (2009).
- [15] A. Nilsson *et al.*, *Science* **308**, 793a (2005).
- [16] J. D. Smith, C. D. Cappa, B. M. Messer, R. C. Cohen, and R. J. Saykally, *Science* **308**, 793b (2005).
- [17] L. G. M. Pettersson, T. Tokushima, Y. Harada, O. Takahashi, S. Shin, and A. Nilsson, *Phys. Rev. Lett.* **100**, 249801 (2008).
- [18] O. Fuchs *et al.*, *Phys. Rev. Lett.* **100**, 249802 (2008).
- [19] M. Odelius, *Phys. Rev. B* **79**, 144204 (2009).
- [20] T. Tokushima, Y. Harada, Y. Horikawa, O. Takahashi, Y. Senba, H. Ohashi, L. G. M. Pettersson, A. Nilsson, and S. Shin, *J. Electron Spectrosc. Relat. Phenom.* **177**, 192 (2010).
- [21] G. N. I. Clark, C. D. Cappa, J. D. Smith, R. J. Saykally, and T. Head-Gordon, *Mol. Phys.* **108**, 1415 (2010).
- [22] A. Nilsson and L. G. M. Pettersson, *Chem. Phys.* **389**, 1 (2011).
- [23] A. Nilsson, T. Tokushima, Y. Horikawa, Y. Harada, M. P. Ljungberg, S. Shin, and L. G. M. Pettersson, *J. Electron Spectrosc. Relat. Phenom.* **188**, 84 (2013).
- [24] M. Cavalleri, H. Ogasawara, L. G. M. Pettersson, and A. Nilsson, *Chem. Phys. Lett.* **364**, 363 (2002).
- [25] M. Cavalleri, M. Odelius, D. Nordlund, A. Nilsson, and L. G. M. Pettersson, *Phys. Chem. Chem. Phys.* **7**, 2854 (2005).
- [26] D. Prendergast and G. Galli, *Phys. Rev. Lett.* **96**, 215502 (2006).
- [27] J. Vinson, J. J. Kas, F. D. Vila, J. J. Rehr, and E. L. Shirley, *Phys. Rev. B* **85**, 045101 (2012).
- [28] C. Huang *et al.*, *Proc. Natl. Acad. Sci. U.S.A.* **106**, 15 214 (2009).
- [29] M. P. Ljungberg, L. G. M. Pettersson, and A. Nilsson, *J. Chem. Phys.* **134**, 044513 (2011).
- [30] M. Neeb, J.-E. Rubensson, M. Biermann, and W. Eberhardt, *J. Electron Spectrosc. Relat. Phenom.* **67**, 261 (1994).
- [31] T. Privalov, F. Gel'mukhanov, and H. Ågren, *Phys. Rev. B* **59**, 9243 (1999).
- [32] F. Gel'mukhanov and H. Ågren, *Phys. Rep.* **312**, 87 (1999).
- [33] F. Hennies, A. Pietzsch, M. Berglund, A. Föhlisch, T. Schmitt, V. Strocov, H. O. Karlsson, J. Andersson, and J.-E. Rubensson, *Phys. Rev. Lett.* **104**, 193002 (2010).
- [34] F. Hennies *et al.*, *Phys. Rev. Lett.* **95**, 163002 (2005).
- [35] L. Braicovich *et al.*, *Phys. Rev. Lett.* **104**, 077002 (2010).
- [36] D. Nordlund, H. Ogasawara, H. Bluhm, O. Takahashi, M. Odelius, M. Nagasono, L. G. M. Pettersson, and A. Nilsson, *Phys. Rev. Lett.* **99**, 217406 (2007).
- [37] See Supplemental Material at <http://link.aps.org/supplemental/10.1103/PhysRevLett.111.193001> for details of the experiment and simulations.
- [38] F. K. Gel'mukhanov, L. N. Mazalov, and A. V. Kondratenko, *Chem. Phys. Lett.* **46**, 133 (1977).
- [39] G. E. Walrafen, M. S. Hokmabadi, and W.-H. Yang, *J. Chem. Phys.* **85**, 6964 (1986).
- [40] M. N. R. Ashfold, J. M. Bayley, and R. N. Dixon, *Chem. Phys.* **84**, 35 (1984).
- [41] J.-J. Max and C. Chapados, *J. Chem. Phys.* **131**, 184505 (2009).
- [42] G. E. Walrafen and E. Pugh, *J. Solution Chem.* **33**, 81 (2004).
- [43] L. Weinhardt, M. Weigand, O. Fuchs, M. Bär, M. Blum, J. D. Denlinger, W. Yang, E. Umbach, and C. Heske, *Phys. Rev. B* **84**, 104202 (2011).
- [44] J. D. Smith, C. D. Cappa, K. R. Wilson, R. C. Cohen, P. L. Geissler, and R. J. Saykally, *Proc. Natl. Acad. Sci. U.S.A.* **102**, 14 171 (2005).
- [45] Y. Nagata, R. E. Pool, E. H. G. Backus, and M. Bonn, *Phys. Rev. Lett.* **109**, 226101 (2012).
- [46] P. Skytt, P. Glans, J.-H. Guo, K. Gunnelin, C. Sâthe, J. Nordgren, F. Gel'mukhanov, A. Cesar, and H. Ågren, *Phys. Rev. Lett.* **77**, 5035 (1996).
- [47] O. Takahashi, M. Odelius, D. Nordlund, A. Nilsson, H. Bluhm, and L. G. M. Pettersson, *J. Chem. Phys.* **124**, 064307 (2006).
- [48] A. Møgelhøj, A. K. Kelkkanen, K. Thor Wikfeldt, J. Schiøtz, J. J. Mortensen, L. G. M. Pettersson, B. I. Lundqvist, K. W. Jacobsen, A. Nilsson, and J. K. Nørskov, *J. Phys. Chem. B* **115**, 14 149 (2011).
- [49] A. Nilsson, C. Huang, and L. G. M. Pettersson, *J. Mol. Liq.* **176**, 2 (2012).